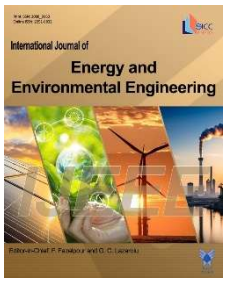

Volume 16, Issue 4, (2025) Article 13

International Journal
of
Energy and Environmental Engineering (IJEEE)

https://doi.org/10.57647/ijeee.2025.1603.13

Synergistic Analysis of Adsorption-Desorption Characteristics Based on Pressure-Desorption Capacity: A Case Study of Xiaohuigou Coal Mine in China

Yongming Zou [1,2], Yaolin Cao [1,2,3], Jie Kang [3], Yuntao Liang [1,3], Congna Hao [4], Linlin Ding [5], Fuchao Tian [1,2,3,*]

[1] *China Coal Research Institute Fushun Branch, Shenfu Demonstration Zone, Liaoning, China*
[2] *State Key Laboratory of Coal Mine Disaster Prevention and Control, China Coal Technology and Engineering Group Shenyang Research Institute, Shenfu Demonstration Zone 113122, China*
[3] *Liaoning Technical University, School of Safety Science and Engineering, Huludao, Liaoning 125100, China*
[4] *Shenyang Urban Construction University, School of Architecture and Planning, Shenyang, Liaoning 110167, China*
[5] *Liaoning University, School of Information, Shenyang, Liaoning 110136, China*

***Corresponding author:** tianfuchao@cumt.edu.cn

Review Article

Received:
07 September 2025
Accepted:
26 November 2025
Published in Issue:
31 December 2025

Abstract

To thoroughly reveal the intrinsic relationships among coal gas adsorption-desorption characteristics, coal structure, and oxidation activity under deep high-temperature and high-pressure conditions, and optimize gas extraction schemes for high-gas mines, we performed a study. Coal samples from the 2201 mining face of No.2 coal seam in Xiaohuigou Coal Mine, China, were selected as the research object. A series of tests were systematically conducted under experimental temperature: 30-120℃, pressure: 0.5-2.5MPa, including proximate analysis, ultimate analysis, adsorption-desorption experiments, thermogravimetric analysis (TG), and Brunauer-Emmett-Teller (BET) pore structure test. The regulatory mechanism of coal gas adsorption and desorption under the coupling effect of temperature and pressure was clarified. The response mechanism between the pore structure of coal samples and their pyrolysis characteristics was determined. An optimization method for gas extraction parameters based on "synergistic regulation of pressure and desorption capacity" was established. This technology was successfully applied to the gas control scenario of the 2201 working face. After applying this technology, the average gas concentration at the upper corner of the working face decreased to 0.40%, with the maximum concentration controlled below 0.67%. The width of the goaf oxidation zone was reduced from the original 40-50 m to 25-30 m. The pure gas extraction flow rate per borehole reached 3.77 m^3/min, equivalent to the extraction effect of 580 Φ113 mm reverse drilling holes. The

cumulative pure gas extraction volume reached 7.01×10^5 m³, which effectively guarantees the safe production during the high-intensity mining of the working face.

Keywords: Adsorption pressure; Gas desorption; Thermogravimetric analysis (TG); Pore structure analysis; Gas extraction

Cite this article: Zou Y., Cao Y., Kang J., Liang Y., Hao C., Ding L., Tian F., Synergistic Analysis of Adsorption-Desorption Characteristics Based on Pressure-Desorption Capacity: A Case Study of Xiaohuigou Coal Mine in China. Int. J. Energy Environ. Eng. 2025; 16(4): Article 13 https://doi.org/10.57647/ijeee.2025.1604.13

1. Introduction

Coal is an important basic energy source in China, accounting for more than 50% of primary energy consumption for a long time[1]. It will continue to dominate China's energy consumption mix for a long time to come. However, with the rapid development of the coal industry, mine gas disasters occur frequently. These disasters seriously threaten the safe production of mines and the life safety of miners. Methane is the primary harmful gas emitted during coal mining operations, and it constitutes the main component of mine gas. Gas not only causes major accidents such as coal mine gas explosions and gas outbursts, leading to casualties and property losses, but also pollutes the atmospheric environment. With the increase in the burial depth of coal seams, gas pressure and emission intensity rise. Especially in deep coal seams, gas control becomes more challenging and the associated risks are significantly higher[2]. According to Document Kuang'an Zong (2024) No. 55 issued by the General Office of the State Administration of Mine Safety Supervision, 9 coal mine gas accidents occurred in 2024, resulting in 55 deaths. Therefore, in-depth investigation into the adsorption and desorption characteristics of coal for gas under pressure conditions is of great significance for mine gas control.

In the field of adsorption and desorption, scholars at home and abroad have conducted extensive research on the adsorption and desorption characteristics of coal. A series of important findings have been obtained. Studies have shown that these characteristics are affected by multiple factors, such as coal rank, coal structure, temperature, pressure, and moisture content. Meanwhile, scholars have established various adsorption and desorption models such as the Langmuir model and Freundlich model, which are used to describe the adsorption and desorption processes of coal.

However, the initial pressure determines the "driving force" of methane in coal pores. The equilibrium pressure reflects the "saturated state" of coal adsorbing methane. The difference in the variation of the two pressures is directly related to coal's adsorption capacity. Traditional studies have focused on the calculation of adsorption capacity. Yet, uneven coal sample density and complex pore structure are prone to causing errors in adsorption capacity. In contrast, pressure changes can directly and accurately characterize the adsorption process. Desorption capacity is the core indicator for evaluating to measure the "recoverability" of coalbed methane. It directly determines gas extraction efficiency and economic benefits. Tian Fuchao et al.[3] independently developed an experimental platform for tracing competitive adsorption-desorption-oxidation coupling disasters in gas-bearing coal. This platform realizes continuous physical simulation of the entire process of competitive adsorption, desorption and spontaneous combustion of multi-component gases under different temperature and pressure working conditions. It provides basic support for the monitoring, early warning, prevention and control of spontaneous combustion of gas-bearing coal in the complex disaster environment of mine goafs. Chen Liuyu et al.[4] studied the pore structure parameters of outburst-prone coal and found that such coal exhibits relatively well-developed pore structures. There are a large number of "ink-bottle" type pores and a small number of closed slit pores, but the pore permeability is poor, resulting in a high residual gas content. Wang Lei et al.[5] found that with the increase of pressure, the fracture structure development of gas-bearing coal is not obvious, and the proportion of isolated pores is large. The connectivity between fractures and isolated pores is poor. Adsorbed gas causes the cracking and failure of coal microstructures through non-mechanical effects, the mechanical effects of swelling stress, and the gas wedge effect by free gas on coal. Shuang Haiqing et al.[6] studied the gas occurrence characteristics in the Chenghe Mining Area. They found that the gas content in the mining area shows an upward trend with the increase of burial depth and coal seam thickness. Tectonic stress is one of the main factors controlling gas occurrence. Xu Huimin[7] analyzed the variation law of gas adsorption and desorption of coal samples with temperature and pressure through

experiments. They found that the gas adsorption capacity of coal samples is negatively correlated with temperature and positively correlated with pressure. Liu Peng et al.[8] found that the gas adsorption and desorption behaviors of coal has changed significantly after being modified via broadband ultrasonic excitation. Yan Min et al.[9] conducted a theoretical analysis of the gas adsorption-desorption-diffusion behaviors of coal. By conducting experiments to investigate the effects of varying temperatures on diffusion coefficients and kinetic diffusion parameters, they found that the higher the temperature, the larger the initial effective diffusion coefficient and kinetic diffusion parameters.

In the field of thermogravimetric analysis (TG), scholars worldwide primarily employ thermogravimetric analyzers to study the pyrolysis characteristics of coal. Thermogravimetric analysis can obtain information such as TG curves and derivative thermogravimetric (DTG) curves of coal at different temperatures. This facilitates an in-depth understanding of the pyrolysis process and mechanism of coal. At present, thermogravimetric analysis has become one of the important methods for studying the pyrolysis characteristics of coal. Li Zhenrong et al.[10] conducted thermogravimetric-infrared spectroscopy (TG-IR) combined experiments. He found that with an increase in adsorption pressure, CH_4 occupies the adsorption sites of coal-oxygen reactions, leading to a reduction in the number of compounds participating in oxidation reactions. Adsorbed CH_4 prevents the oxidation of some organic matter in coal and inhibits coal oxidation. Mohalik NK et al.[11] analyzed 80 coal samples from Indian coalfields using TG and found that in the temperature range of 150-350℃, oxygen adsorption leads to an increase in coal sample mass. Selcuk Nevin et al.[12] studied the combustion of coal in O_2/N_2 and O_2/CO_2 atmospheres using TG-IR, and found that the type and concentration of external gases have almost the same impact on the pyrolysis evolution of coal.

In the field of BET experiments, scholars worldwide primarily employ BET specific surface area analyzers to determine the specific surface area and pore structure of coal. BET experiments can determine key parameters including the specific surface area, pore volume, and pore size distribution of coal samples. This lays an important foundation for investigating coal's adsorption-desorption characteristics and gas migration laws. Li et al.[13] found through BET experiments that the pore volume and specific surface area of coal samples decrease monotonically with an increase in temperature and pressure. Meanwhile, the proportion of micropores and mesopores that facilitate coal-oxygen reactions shows an upward trend. Zhou Xiaoqing[14] conducted experiments and found that with the increase of degassing temperature for anthracite, a large number of pores are exposed. This leads to a significant increase in pore structure parameters (i.e., BET specific surface area, total pore volume, and adsorption capacity), while the average pore diameter continuously decreases. Zhou Ya[15] found through liquid nitrogen adsorption experiments that in terms of gas-bearing properties: for high-rank coal, Langmuir pressure and Langmuir volume generally show an upward trend with increasing coal maturity. For medium-rank coal, the correlation between its pore volume and Langmuir volume/Langmuir pressure is not statistically. With the increase of BET specific surface area, the Langmuir volume of medium-rank coal exhibits a weak positive correlation with this parameter, while Langmuir pressure shows a negative correlation. Li Xijian[16] took tectonic coal and primary-structured coal from Qinglong Coal Mine, Xiaotun Coal Mine (located in Bijie), and coal mines in the Liupanshui area as research objects. He studied the pore characteristics of the two types of coal. The results show that tectonic coal has a larger BET specific surface area, a smaller pore diameter, and a higher desorption capacity than primary structure coal, which has a significant impact on adsorption-desorption characteristics.

As one of China's important coal production bases, Xiaohuigou Coal Mine also faces severe gas problems during coal mining. The coal mine is characterized by high gas content, high gas pressure, and unstable gas emission intensity. Therefore, this paper takes Xiaohuigou Coal Mine as the research subject, and collects coal samples to conduct proximate analysis. Moisture content, ash content, volatile matter content, and fixed carbon content of coal samples were determined to understand their basic properties. Meanwhile, ultimate analysis experiments were conducted to measure the contents of carbon, hydrogen, oxygen and other elements in coal samples, so as to analyze their elemental composition. Adsorption-desorption experiments were carried out to study the adsorption-desorption characteristics of coal samples under different pressure conditions. Thermogravimetric experiments (TG) were performed to analyze the pyrolysis characteristics and mechanism of coal samples. BET experiments were conducted to determine the specific surface area and pore structure of coal samples, and to explore the influence of pore structure on gas adsorption-desorption characteristics.

Most existing studies have focused on the effects of a single factor on coal gas adsorption-desorption characteristics, or been limited to the correlation analysis between coal structure and oxidation activity under

conventional temperature and pressure conditions. In contrast, few studies have conducted research on the synergistic effects among coal gas adsorption-desorption characteristics, coal structure, and oxidation activity under deep high-temperature and high-pressure environments. Additionally, the coupling mechanism between laboratory test results and the optimization of field gas extraction parameters has not yet been established. On the contrary, this study takes the 2201 working face of Xiaohuigou Coal Mine as the engineering background, integrates multiple characterization methods, and realizes the cross-scale correlation analysis of coal structure-oxidation activity-adsorption-desorption behavior. This study aims to enhance the utilization efficiency of gas resources in the coal mine and provide theoretical support and engineering reference for optimizing gas extraction parameters in deep high-gas coal mines and ensuring the safe and efficient mining of coal mines.

2. Experimental Apparatus and Scheme

2.1. Experimental Materials and Pretreatment

The coal samples employed in this experiment were sampled from the 2201 working face of No. 2 coal seam in Xiaohuigou Coal Mine. This working face is located in the eastern wing of the No.1 mining area. It is one of the main mining faces of the coal mine and exhibits good representativeness.

First, the collected coal samples were pretreated to remove surface impurities and adherent gangue. Then, the coal samples were crushed to a particle size of less than 25 mm to facilitate subsequent experimental operations. Crushing was performed using a jaw crusher, and the discharge particle size of the crusher was controlled to ensure it meets the requirements.

During the crushing process, attention was paid to controlling the crushing duration and rotational speed, which avoided changes in the properties of the coal samples caused by frictional heating. The crushed coal samples were sieved with a standard sieve. Coal samples within the particle size fraction of 0.2-0.25 mm were selected for subsequent experiments[17]. Specifically, 10 g of coal samples in this particle size range were weighed for each set of experiments. Coal samples in this particle size range have a large specific surface area, which can better reflect the adsorption and desorption characteristics of coal. Finally, the sieved coal samples were sealed in airtight containers and stored in a low-temperature, dark, and dry environment to prevent moisture absorption and oxidation that may alter the coal sample properties for later use.

2.2. Design and Construction of Experimental Apparatus

The adsorption-desorption experiments were conducted using a self-developed intelligent gas adsorption-desorption testing apparatus. The apparatus consists of four main parts: the gas supply system, the adsorption-desorption system, the vacuum pumping system, and the data acquisition and storage system. The schematic diagram of the experimental apparatus is shown in Figure 1.

2.3. Experimental Methods and Procedures

(1) Proximate Analysis

Proximate analysis was performed using a proximate analyzer. The instrument integrates a far-infrared heating device with an electronic balance. It measures the mass change of coal samples during heating under specific atmospheric conditions, temperatures, and heating durations.

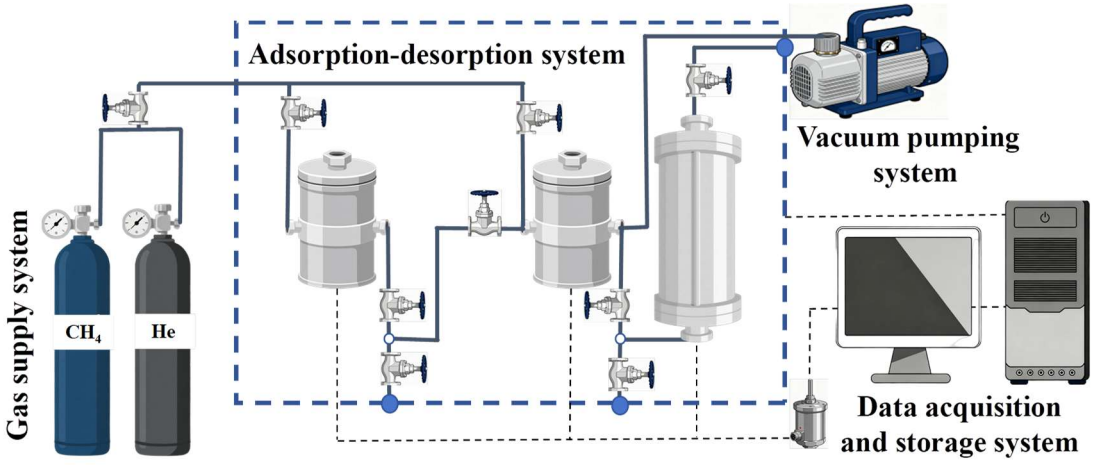

Figure 1. Schematic diagram of intelligent test device for competitive adsorption of multiple gases under variable temperature conditions

Based on this, proximate analysis indicators such as moisture, ash, and volatile matter of coal samples were calculated. For moisture determination: The temperature was raised to approximately 145 ℃ and held isothermal for 20 minutes. The moisture analysis ends when the change in crucible mass did not exceed the system's set value. For volatile matter determination: The temperature of the high-temperature furnace was raised to 900 ℃. Determination was carried out after maintaining the constant temperature for a specified duration. For ash determination: The temperature was further increased again to 850 ℃ and maintained constant. The ash analysis ends when the change in crucible mass did not exceed the system's set value.

(2) Ultimate Analysis

Ultimate analysis was performed using an ultimate analyzer. Its working principle is based on the combustion method. Coal samples were burned in a high-temperature oxygen flow, converting elements such as carbon, hydrogen, and nitrogen in coal into corresponding oxides. Subsequently, chromatographic separation and detection technology was used to determine the content of each element. The instrument has a measurement accuracy of ±0.1% for carbon, hydrogen, and nitrogen, respectively.

(3) Adsorption-Desorption Experiments

An intelligent gas adsorption-desorption testing apparatus (Model: TZX-3000) was used. The gas used in the experiments was methane with a purity of 99.99%. Gas at different pressure levels was injected into the adsorption tank containing coal samples. After reaching adsorption equilibrium, the pressure was gradually reduced. The volume change of gas during desorption was measured to characterize the gas adsorption-desorption behaviors of the coal samples. The instrument has a pressure measurement range of 0-10MPa (with an accuracy of ±0.1MPa) and a volume measurement accuracy of ±0.01 cm^3.

(4) Thermogravimetric Analysis (TG)

A thermogravimetric analyzer (Model: STA6000) was utilized. High-purity air was used as the heating atmosphere, with a gas flow rate of 50 mL/min. Under programmed temperature heating conditions, the mass change of the prepared coal samples during heating was measured. This facilitated the acquisition of the pyrolysis characteristics and underlying mechanism of coal samples. The instrument's temperature range is from room temperature to 1000 ℃. The heating rate can be adjusted within 1-50 ℃/min, and the mass measurement accuracy is ±0.01 mg.

(5) BET Analysis

A physical adsorption analyzer (Model: ASAP2020) was used for BET analysis. Operating on the principle of liquid nitrogen adsorption, the adsorption capacity of nitrogen onto the surfaces of the prepared coal samples under different relative pressures was measured. The specific surface area and pore structure of coal samples are calculated via the BET equation. The instrument has a specific surface area measurement range of ≥0.0005 m^2/g, a pore diameter measurement range of 1.7-300nm, and a minimum pore volume detection limit of 0.0001 m^3/g. The schematic experimental flowchart is shown in Figure 2.

3. Results and Analysis

3.1. Basic Characterization Results of Coal Samples

3.1.1. *Proximate Analysis*

The proximate analysis was conducted on coal samples collected from Xiaohuigou Coal Mine. The results are shown in Table 1. It can be observed that the proximate analysis indicators of the coal sample exhibit a "three lows and one high" pattern: low moisture, low ash, low volatile matter, and high fixed carbon. The moisture content is 1.04%, thus classifying the coal as ultra-low moisture coal. This indicates a dry occurrence setting of the coal. The free water and bound water in the pores are extremely limited. This can reduce the blockage of gas diffusion channels and directly optimize the adsorption-desorption process. The ash content is 5.24%, which meets the low ash coal classification standard (A < 10%). The coal is high-quality thermal coal and chemical coal. The content of inorganic minerals such as SiO_2 and Al_2O_3 in the coal is low. This low ash content not only reduces the interference of minerals on pyrolysis characteristics in TG experiments but also prevents the invalid filling of pores in BET experiments, ensuring the accuracy of the determination of parameters such as specific surface area. The volatile matter content is 11.86%, falling within the low volatile matter range (V < 20%). Combined with the high fixed carbon characteristic, it can be judged that the coal sample has a high degree of metamorphism, close to the category of lean coal or meager coal. Its molecular characteristics—a well-developed aromatic ring structure and a limited number of side chain groups—will directly affect gas adsorption capacity and pyrolysis reaction activity. The fixed carbon content is 87.35%, significantly higher than the 60%-80% range for conventional bituminous coal. As the core of combustible organic matter in coal, the high content ensures a stable coal matrix skeleton and a well-developed, regular pore structure. It not only provides abundant active sites for the adsorption of gas molecules but also lays a material foundation for stable combustion in the high-temperature phase of TG experiments. These characteristics collectively determine the basic physical and chemical properties of the coal sample.

10.57647/ijeee.2025.1603.13

Table 1. Results of proximate analyzes of the coal

Analysis Items	Content（ad, %）
Mad	1.04
Aad	5.24
Vad	11.86
FCad	87.35

Note: "ad" is the abbreviation of air-dried basis, which complies with the standard terminology for coal analysis.

Table 2. Results of ultimate analyzes of the coal

Analysis Items	Content（ad, %）
C	89.32
H	3.76
N	1.40

Note: "ad" is the abbreviation of air-dried basis, which complies with the standard terminology for coal analysis.

3.1.2. *Elemental Analysis*

Elemental analysis was performed on coal samples from Xiaohuigou Coal Mine using an ultimate analyzer. The results are shown in Table 2. The elemental composition of the coal sample exhibits a "high carbon, medium hydrogen, and low nitrogen" characteristic. This characteristic is highly consistent with the conclusion regarding the high degree of metamorphism revealed by proximate analysis. The carbon content reaches 89.32%, significantly higher than that of typical conventional bituminous coal (75%-85%) and close to the category of anthracite. As the dominant component of organic matter, carbon predominantly exists in the form of highly condensed aromatic ring structures. It is the core source of the stable coal skeleton and active sites for gas adsorption. The hydrogen content is 3.76%, placing it in the transition zone between bituminous coal and anthracite. Hydrogen is mainly bonded to aliphatic side chains and bridge bonds. Despite the high metamorphism degree, some short-chain aliphatic structures are still retained. This provides a material basis for the generation of pyrolytic volatile matter and gas desorption. The nitrogen content is 1.40%, thus classifying the coal as low-nitrogen coal. Nitrogen in the coal mainly exists in heterocyclic forms such as pyrrole and pyridine. It originates from nitrogen-containing components such as proteins in coal-forming plants. Its content is affected by both the original coal-forming materials and the degree of metamorphism.

Combined with the results of proximate and elemental analysis, the coal sample from Xiaohuigou Coal Mine can be categorized as a high-metamorphism coal, close to lean coal or meager coal. This coal rank is closely correlated with its gas adsorption potential. Specifically, the high fixed carbon content (87.35%, proximate analysis) and high carbon content (89.32%, elemental analysis) indicate a well-developed condensed aromatic ring structure in the coal matrix. This structure not only forms a stable pore skeleton but also provides abundant active adsorption sites for gas molecules, enhancing the physical adsorption capacity of coal. Meanwhile, the low volatile matter content (11.86%) reflects the limited number of aliphatic side chains in the coal, which reduces the competitive adsorption of volatile components on gas molecules and further optimizes the gas adsorption process. The low ash content (5.24%) avoids the invalid filling of pore channels, ensuring smooth gas diffusion and adsorption-desorption dynamics. In addition, the medium hydrogen content (3.76%) indicates the retention of a small amount of short-chain aliphatic structures, which can promote the desorption of adsorbed gas under the action of external factors (e.g., temperature rise, pressure drop). In summary, the coal rank determined by proximate and elemental analysis is the intrinsic factor controlling the gas adsorption-desorption potential of the coal sample.

3.2. Analysis of Adsorption-Desorption Experimental Results

3.2.1. *Changes in Adsorption Pressure*

Adsorption experiments were conducted on coal samples from Xiaohuigou Coal Mine. The adsorption pressure variation curves under different temperature conditions were obtained, as shown in Figure 3.

By analyzing the adsorption pressure variation characteristics under different initial pressures presented in Figure 3, it can be concluded that under the same temperature condition, the higher the initial pressure, the higher the resulting adsorption equilibrium pressure. For example, at 30 ℃, when the initial pressure increases from 0.5MPa to 2.5MPa, the adsorption equilibrium pressure rises from 0.45MPa to 2.26MPa. This is because a higher initial pressure provides a stronger driving force for gas molecules to diffuse into the pores of the coal matrix. A greater number of gas molecules are adsorbed onto the coal surface, leading to a higher system pressure at equilibrium.

Regarding the influence of temperature on adsorption pressure, under the same initial pressure, the adsorption equilibrium pressure shows an upward trend with increasing temperature. Taking an initial pressure of 1.0 MPa as an example: when the temperature rises from 30 ℃ to 120 ℃, the adsorption equilibrium pressure increases from 0.88MPa to 0.95MPa. This is because elevated temperature weakens the adsorption interactions between gas molecules and the coal matrix surface. It diminishes the gas adsorption capacity of coal[18, 19], resulting in a higher system pressure at

adsorption equilibrium. This temperature-induced inhibitory effect on gas adsorption is more significant under high initial pressures.

In addition, it was found during the experiment that the time required for the adsorption pressure to reach equilibrium increases with increasing initial pressure and decreases with rising temperature. At low initial pressure (e.g., 0.5MPa), adsorption equilibrium is achieved in approximately 60 minutes at 30 ℃, while the adsorption equilibrium time extends to more than 120 minutes at an initial pressure of 2.5MPa. Under the same initial pressure, the equilibrium time at 120 ℃ is 30-40% shorter than that at 30 ℃. This is because gas molecules need more time to diffuse into the deep pores of the coal under high initial gas pressure conditions. In contrast, elevated temperatures accelerate the thermal motion of gas molecules, shortening the adsorption equilibrium time.

3.2.2. *Changes in Desorption Capacity*

Desorption experiments were conducted on the prepared coal samples from Xiaohuigou Coal Mine. The adsorption-desorption curves under different temperature and pressure conditions were obtained, as presented in Figure 4.

By analyzing the desorption capacity variation characteristics under different temperatures in Figure 4, it can be concluded that desorption capacity exhibits the characteristic of "rapid-growth and gradual-stabilization" with the extension of desorption time. In the initial stage of desorption (0-20 min), gas molecules are rapidly desorbed from the coal surface and large-diameter pores, leading to a sharp rise in desorption capacity[20]. After 20 min, the desorption rate gradually declines. The desorption capacity basically reaches a state of desorption equilibrium after 60 min. This is because the free and weakly adsorbed gas molecules, which are amenable to rapidly desorption, accounts for a high proportion in the initial stage. In the later stage, desorption is dominated by strongly adsorbed gas, which requires overcoming a higher adsorption energy barrier specific to strongly adsorbed gas[21, 22].

It can be observed from the experimental results that temperature has a significant impact on desorption capacity. At the same desorption duration and initial gas pressure, the higher the temperature, the lower the desorption capacity. Compared with 30 ℃, the gas desorption capacity of the prepared coal samples at five preset pressure points exhibits a significant reduction at 60 ℃, 90 ℃, and 120 ℃. The corresponding desorption capacities decrease by 2.34%, 3.11%, 2.99%, 4.76%, 3.98%; 12.94%, 8.23%, 4.62%, 12.14%, 8.96%; and 20.35%, 11.68%, 6.73%, 14.99%, 13.94% respectively.

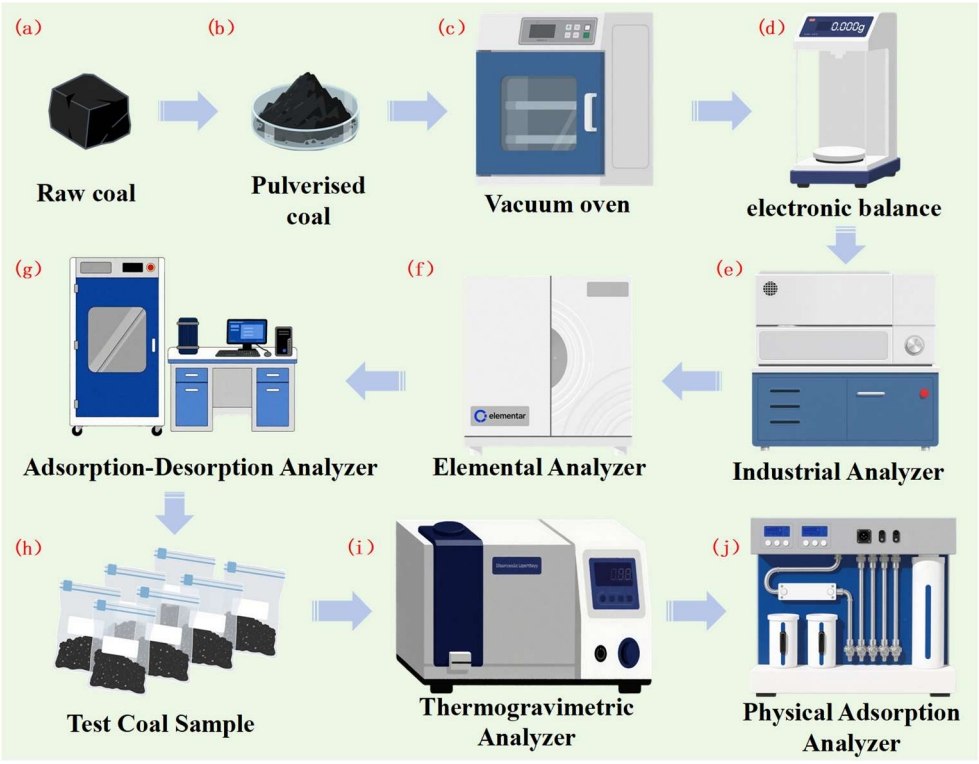

Figure 2. Experimental flow chart.

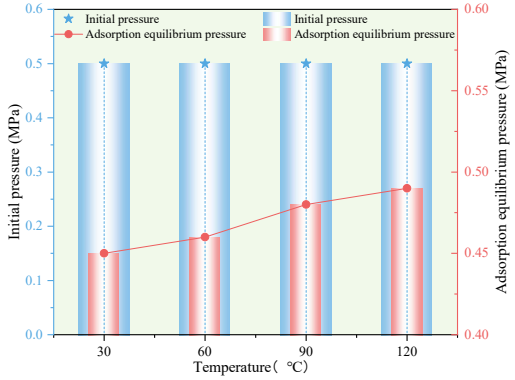

(a) 0.5MPa

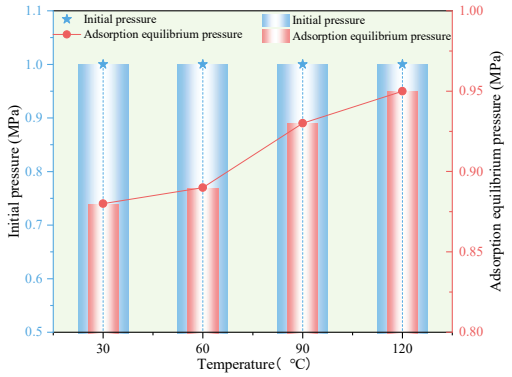

(b) 1.0MPa

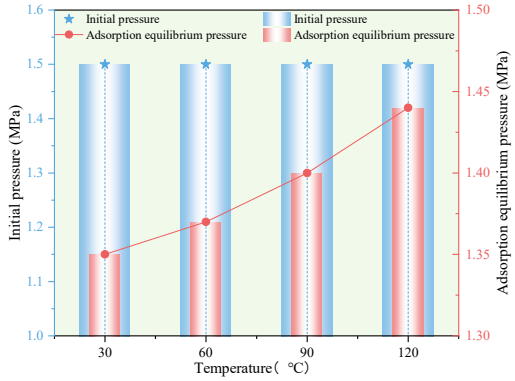

(c) 1.5MPa

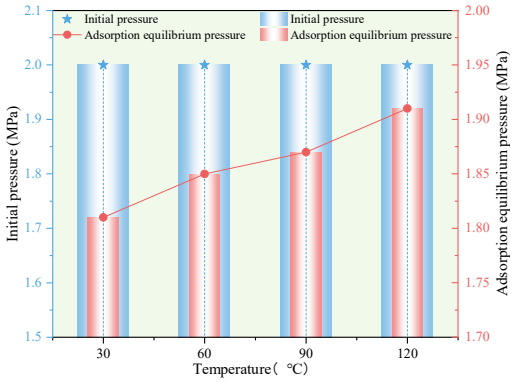

(d) 2.0MPa

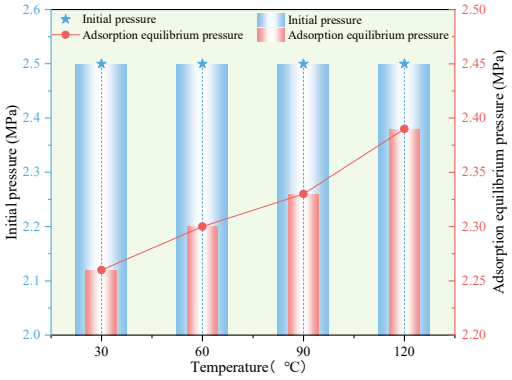

(e) 2.5MPa

Figure 3. Adsorption pressure diagram

10.57647/ijeee.2025.1603.13

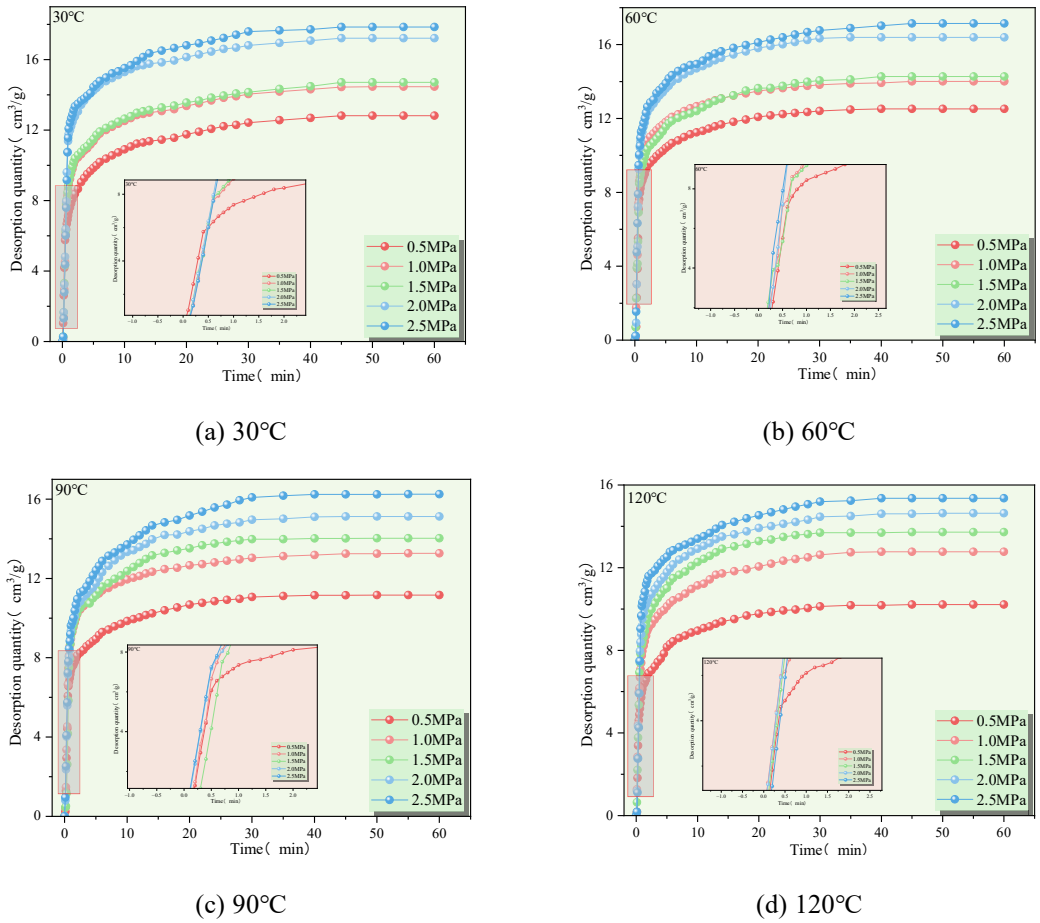

(a) 30℃ (b) 60℃

(c) 90℃ (d) 120℃

Figure 4. Desorption capacity diagram

Compared with 60 ℃, the desorption capacities at 90 ℃ and 120 ℃ decrease by 10.86%, 5.28%, 1.68%, 7.75%, 5.19% and 18.45%, 8.85%, 3.85%, 10.74%, 10.37% across the five preset pressure points. Compared with 90 ℃, the desorption capacity at 120 ℃ decreases by 8.51%, 3.77%, 2.21%, 3.24%, 5.47% across the five preset pressure points. From the above analysis, it is clear that temperature significantly affects the gas desorption behavior of the coal matrix. With an increase in adsorption temperature, the inhibitory effect on the gas desorption capacity of coal tends to intensify[23]. This is because desorption is the reverse process of physical adsorption.

Under constant pressure, an increase in temperature reduces adsorption capacity, while a decrease in temperature enhances adsorption capacity. Therefore, adsorption capacity decreases with the increase of adsorption temperature, thus leading to a corresponding reduction in the volume of gas desorbed at ambient temperature. Meanwhile, combined with the coupling relationship between initial adsorption pressure and desorption capacity, it can be seen that the higher the initial adsorption pressure, the higher the corresponding desorption capacity. The desorption capacities of the coal sample at four temperature points at an initial pressure of 0.5MPa are 12.82 cm³/g, 12.52 cm³/g, 11.16 cm³/g, and 10.21 cm³/g. At 2.5MPa, the desorption capacities at the four temperature points are 17.85 cm³/g, 17.14 cm³/g, 16.25 cm³/g, and 15.36 cm³/g. Compared with the desorption capacity under 0.5MPa, they increase by 39.24%, 36.9%, 45.61%, and 50.44% respectively. This is because coal adsorbs a greater total amount of gas under high initial pressure, resulting in higher volume of desorbable gas. Combined with the actual detection results of gas composition in underground goafs, the gas present in such environments is mainly air and methane. It is worth noting that the increase in temperature and pressure directly affects the occurrence state of gas in coal. The increase of both inhibits the gas desorption process in coal, leading to a decrease in gas desorption capacity.

3.3. Analysis of Thermogravimetric Results

Thermogravimetric experiments were conducted on coal samples from Xiaohuigou Coal Mine that were subjected to different adsorption temperature and pressure conditions using a thermogravimetric analyzer (TGA).

The experiments were performed in a high-purity air atmosphere, which is the prerequisite for defining the combustion stage of coal samples and avoiding misunderstandings about the reaction process. The acquired thermogravimetric (TG) curves and derivative thermogravimetric (DTG) curves are shown in Figure 5, Figure 6, and Figure 7.

From the TG-DTG curves of raw coal sample in Figure 5, it can be seen that the pyrolysis process of the coal sample can be divided into three stages: drying and dehydration stage (room temperature-200 ℃), pyrolysis weight loss stage (200-600 ℃), and char combustion stage (600-800 ℃)[24-26]. The weight loss rate in the drying and dewatering stage is only 1.0-1.5%. This low weight loss rate is consistent with the ultra-low moisture content of 1.04% determined via proximate analysis. It indicates that the content of free water and bound water in the coal sample is extremely low. The pyrolysis weight loss stage is the main weight loss interval, with a weight loss rate of 28-30%. Reactions such as cleavage of aliphatic side chains, ring-opening of aromatic structures, and release of volatile matter occur mainly in this stage. A distinct maximum weight loss rate peak appears at approximately 465 ℃ on the DTG curve. This corresponds to the temperature of concentrated volatile matter release. The weight loss rate in the char combustion stage is about 40-42%. The fixed carbon fraction reacts with oxygen to form CO_2 and CO in this stage. The weight loss profile is relatively gentle, reflecting the stable combustion characteristics of the high fixed carbon coal sample.

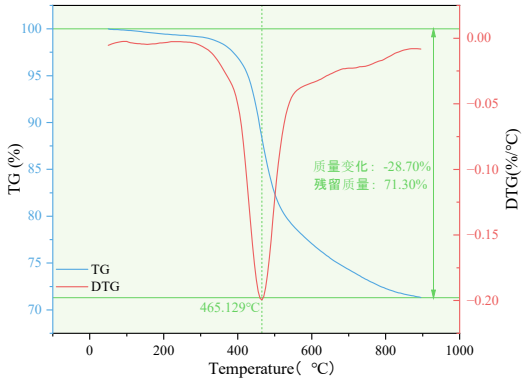

Figure 5. Raw coal TG-DTG curves

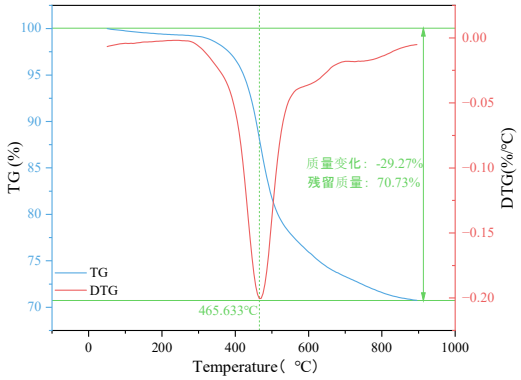

(a) 30-2.5

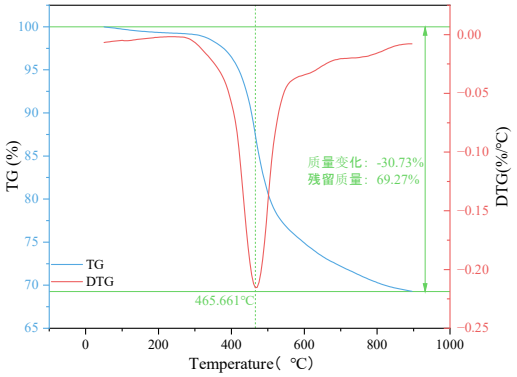

(b) 60-2.5

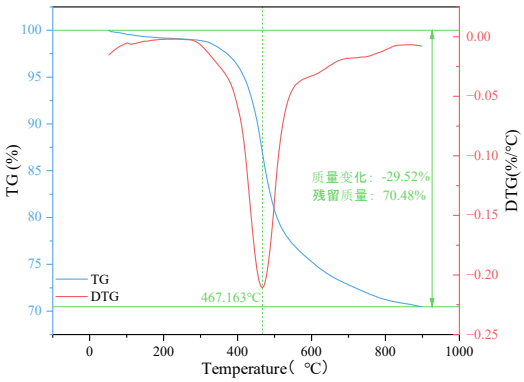

(c) 90-2.5

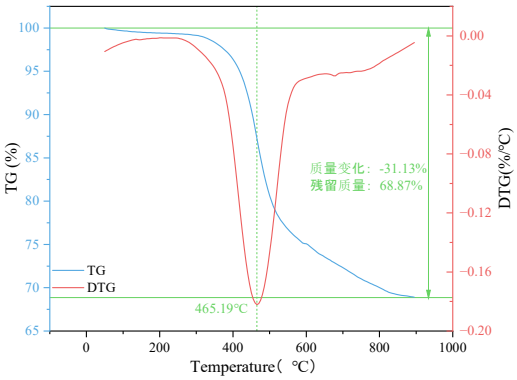

(d) 120-2.5

Figure 6. TG-DTG curves at different adsorption temperatures

By analyzing the TG-DTG curves under different adsorption temperatures in Figure 6, it can be concluded that adsorption temperature has a significant impact on the pyrolysis characteristics of the coal sample. As the adsorption temperature increases from 30 ℃ to 120 ℃, the pyrolysis weight loss rate exhibits a gradual increasing trend. The total weight loss rate is 29.27% at 30 ℃ and increases to 31.13% at 120 ℃. This is because during high-temperature adsorption, gas desorption induces alterations in the pore structure of the coal matrix (e.g., fracture development)[27]. It Such pore structure alterations augment the contact area between oxygen and active sites within the coal matrix, promoting pyrolysis and combustion reactions[28]. The temperature corresponding to the maximum weight loss rate peak on the DTG curve decreases slightly with increasing adsorption temperature. This temperature measures 465.633 ℃ at 30 ℃ and decreases to 465.19 ℃ at 120 ℃. This indicates that the chemical structure of coal is more prone to decomposition after high-temperature adsorption, accompanied by a slight reduction in thermal stability. In addition, the higher the adsorption temperature, the lower the weight loss rate in the char combustion stage. This suggests that high-temperature adsorption may cause some strongly adsorbed gas to remain in the coal micropores, inhibiting the reaction between char and oxygen.

From the TG-DTG curves under different adsorption pressures in Figure 7, it can be seen that the influence of adsorption pressure on the pyrolysis weight loss characteristics of the coal sample differs from that of temperature. As the adsorption pressure increases from 0.5 MPa to 2.5 MPa, the total pyrolysis weight loss rate exhibits a fluctuating trend of decreasing first, then increasing, followed by a subsequent decrease. It is 31.99% at 0.5 MPa, 30.03% at 1.0 MPa, drops to 29.59% at 1.5 MPa, rises to 32.09% at 2.0 MPa, and falls again to 29.52% at 2.5 MPa. Under low pressures (0.5-1.5 MPa), an increase in pressure enhances the adsorption affinity of gas molecules within the coal pores. These adsorbed gas molecules occupy some reactive sites, inhibits pyrolysis reactions, and leads to a decrease in weight loss rate. Under high pressures (1.5-2.5 MPa), excessively high pressure induces compression deformation of the coal matrix pore structure. Some micropores are converted into mesopores. Meanwhile, the desorption of more adsorbed gas molecules damages the coal structure and increases reactive active sites, thereby promoting pyrolysis reactions and increasing the weight loss rate. The temperature of the maximum weight loss rate peak on the DTG curve does not change significantly with adsorption pressure. It is basically stable between 465-467 ℃, indicating that adsorption pressure has little effect on the main reaction temperature of coal pyrolysis[29]. However, under high pressures (2.0-2.5 MPa), the DTG peak profile becomes broader. This indicates that the temperature interval for pyrolysis reactions is broadened. The structural damage to the coal matrix induced by the gas adsorption-desorption process rendering the pyrolysis reactions of different reactive sites more kinetically dispersed.

3.4 Analysis of BET Results

3.4.1. *Adsorption-Desorption Curves*

The adsorption-desorption curves of the coal samples are shown in Figure 8. Analysis of the curve characteristics of coal samples after adsorption and desorption under different temperatures and pressures reveals that all curves exhibit the features of Type IV adsorption isotherms with distinct hysteresis loops. This indicates that the coal samples are predominantly composed of mesopores and macropores, with well-developed pore structures. The hysteresis loops are characteristic of Type H4, suggesting the presence of slit-shaped and ink-bottle-shaped pores within the coal matrix in the coal samples. Such pore structures can result in the entrapment of nitrogen molecules within the coal matrix pores during desorption, leading to a distinct separation between the desorption and adsorption branches of the isotherms. Under an adsorption pressure of 0.5MPa, the low-temperature nitrogen adsorption capacities of coal samples treated at 30 ℃, 60 ℃, 90 ℃, and 120 ℃ are 6.346 cm^3/g, 5.545 cm^3/g, 5.725 cm^3/g, and 5.696 cm^3/g, respectively. Compared with the adsorption capacities under 1.5 MPa (3.591 cm^3/g, 4.034 cm^3/g, 3.525 cm^3/g, 3.962 cm^3/g), they are higher than those at 43.41%, 27.25%, 38.43%, and 30.44% respectively. Compared with the adsorption capacities under 2.5 MPa (2.499 cm^3/g, 2.319 cm^3/g, 1.456 cm^3/g, 2.279 cm^3/g), they decrease by 60.62%, 58.17%, 74.57%, and 59.99% respectively. This is because under low pressure (0.5 MPa), the pore structure of the coal matrix does not undergo significant compressive deformation. The connectivity of micropores (< 2nm) and mesopores (2–50nm) is good, allowing nitrogen molecules to fully diffuse and adsorb on the pore surfaces, resulting in higher adsorption capacity. Under high pressures (1.5 MPa and 2.5 MPa), the effective stress on coal increases, leading to a pore compression effect: micropores undergo closure, and the throats of mesopore become constricted, and the specific surface area and pore volume of the coal matrix decrease[30].

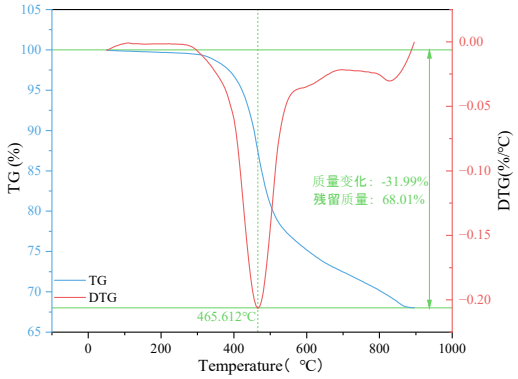

(a) 90-0.5

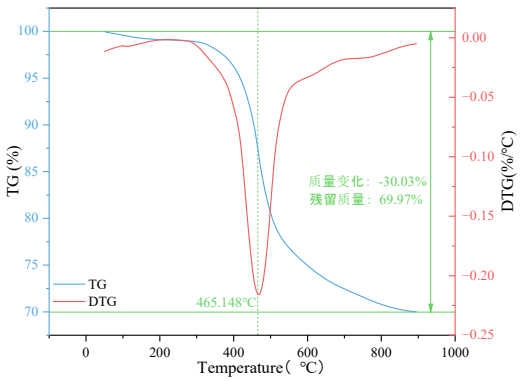

(b) 90-1

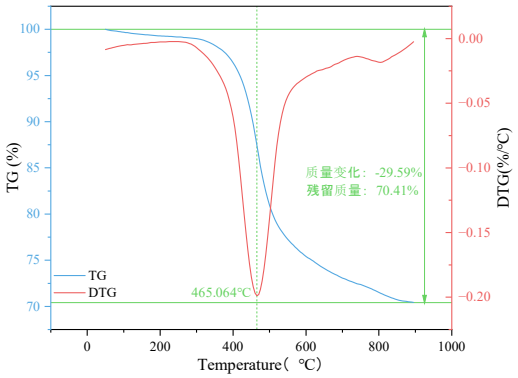

(c) 90-1.5

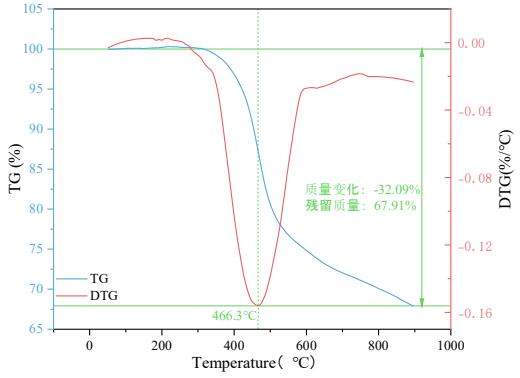

(d) 90-2

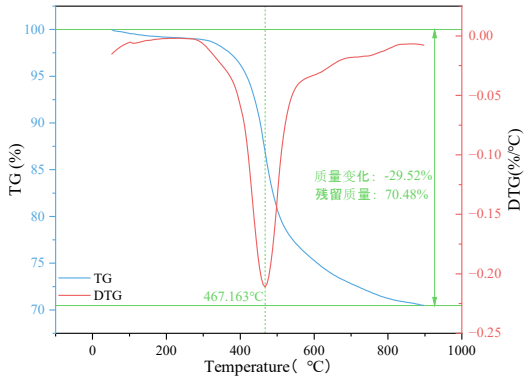

(e) 90-2.5

Figure7. TG-DTG curves at different adsorption pressures

The diffusion resistance of nitrogen molecules increases. Even with increasing pressure, the number of effectively available adsorption sites within the pores decreases, resulting in a substantial reduction in adsorption capacity.

The higher the pressure, the more intense the pore compression: the coal pore structure is more severely damaged under 2.5 MPa (especially the 90 ℃ treatment group, with a decrease of 74.57%). Thus, the adsorption capacity is further reduced compared with 1.5MPa, and the average reduction rate nearly doubles (average decrease rate from 34.88% to 63.34%). Experimental data show that the adsorption capacity reaches the minimum value of 1.456 cm^3/g with the largest decrease (74.57%) under the 90 ℃-2.5 MPa combination. This reflects that adsorption temperature pretreatment enhances the pressure sensitivity of coal pores: high-temperature treatment may impair the mechanical strength of the coal matrix skeleton, making the pore structure more prone to compression under high

pressure, resulting in the most significant loss of adsorption sites. In contrast, the adsorption capacity of the 60 ℃ treatment group is relatively stable under all pressures. This may be because this temperature not only eliminates excess moisture but also does not damage the coal skeleton structure, achieving "optimization" of the pore structure.

3.4.2. *Specific Surface Area and Pore Volume*

The specific surface areas and pore volumes of coal samples subjected to adsorption-desorption cycles under different temperature and pressure conditions are presented in Figure 9 and Figure 10.

From the pore specific surface area data under different adsorption temperatures and pressures in Figure 9, it can be seen that the specific surface area of the coal sample is mainly contributed by micropores and mesopores.

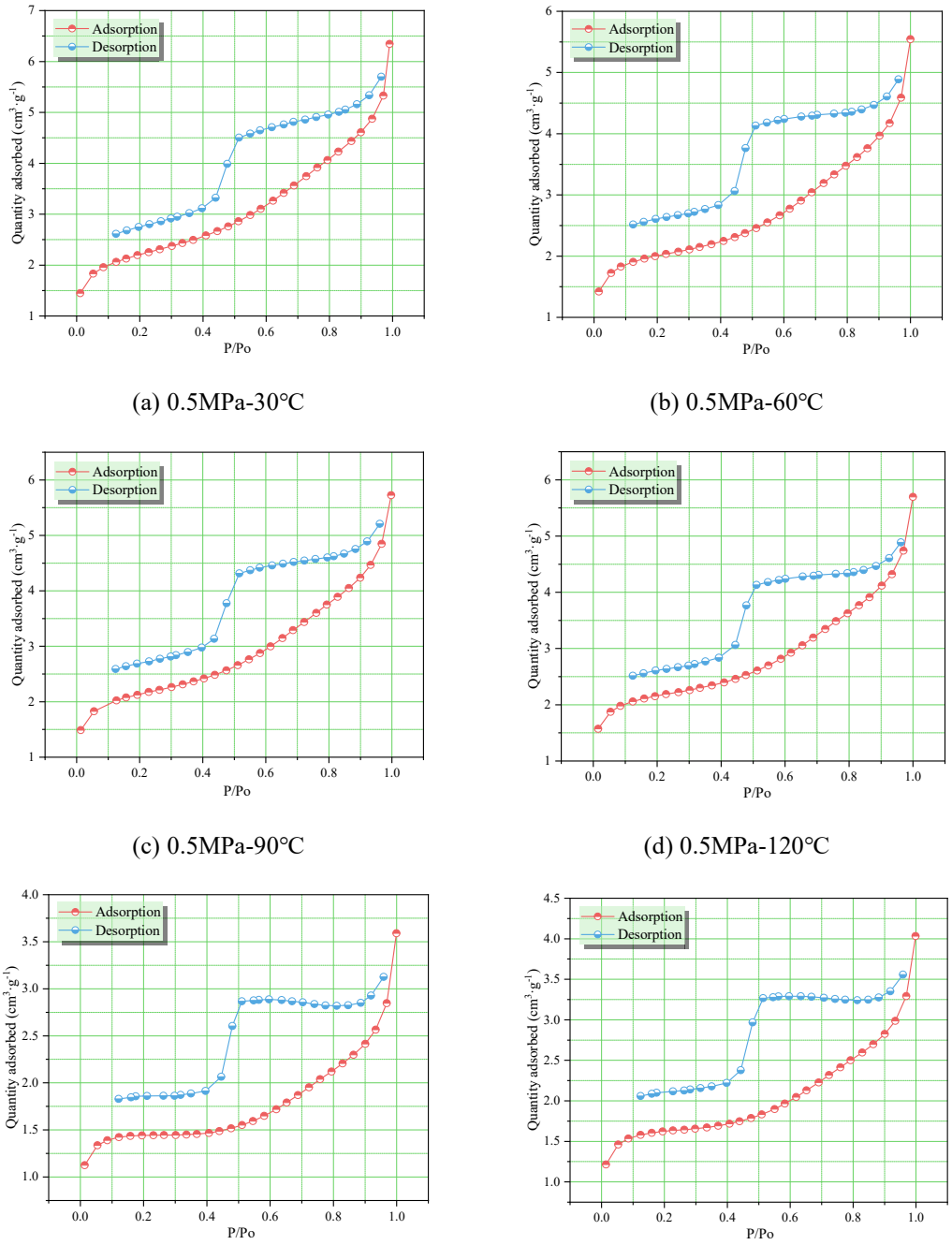

(a) 0.5MPa-30℃ (b) 0.5MPa-60℃

(c) 0.5MPa-90℃ (d) 0.5MPa-120℃

(e) 1.5MPa-30℃ (f) 1.5MPa-60℃

Figure 8. Adsorption-desorption curves

10.57647/ijeee.2025.1603.13

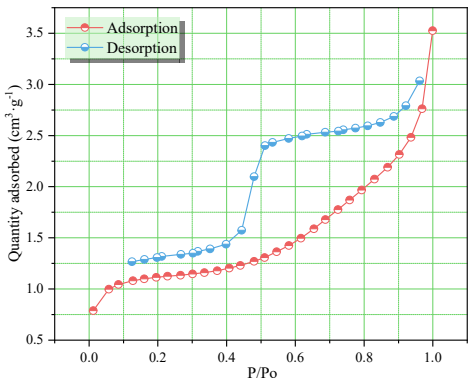

(g) 1.5MPa-90℃

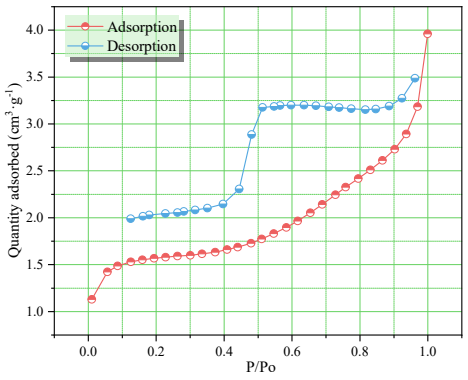

(h) 1.5MPa-120℃

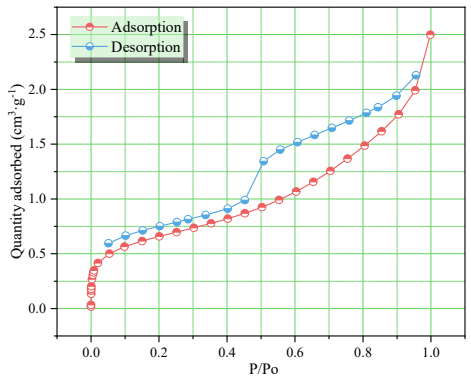

(i) 2.5MPa-30℃

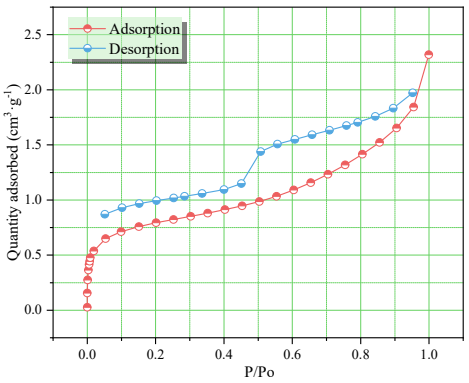

(j) 2.5MPa-60℃

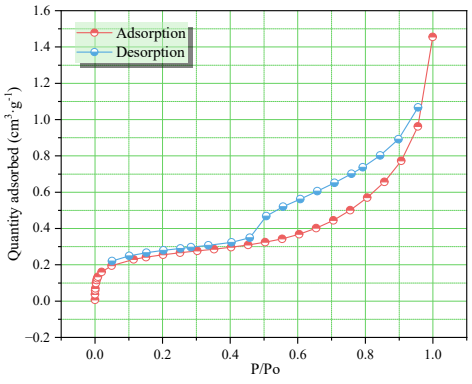

(k) 2.5MPa-90℃

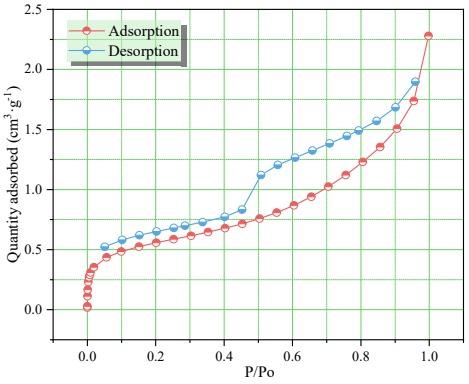

(l) 2.5MPa-120℃

Figure 8. Adsorption-desorption curves(continued)

Macropore contribute less than 10% to the total specific surface area of the coal matrix. The effect of temperature on the specific surface area of different pores with different size fractions varies: as the temperature increases from 30 ℃ to 120 ℃, the micropore specific surface area shows a decreasing trend—measuring approximately 0.896 m²/g at 30 ℃ and decreasing to 0.753 m²/g at 120 ℃.

This is because high temperature causes shrinkage or collapse of coal micropores, reducing the number of micropores. Mesopores have both a high specific surface area and favorable pore connectivity, serving as the main site for nitrogen molecule diffusion and adsorption[31]. Data show that the mesopore adsorption capacity is the highest under all temperature-pressure combinations (reaching 4.315 m²/g at 30 ℃/0.5 MPa), and its variation trend is highly consistent with the total adsorption capacity (e.g., mesopore adsorption capacity under 1.5 MPa: 30 ℃ > 60 ℃ > 120 ℃ > 90 ℃). This confirms that mesopores are the core pore size range affecting coal adsorption capacity. The macropore specific surface area is less affected by temperature, basically stable at around

0.1 m²/g. The influence of pressure on pore specific surface area is as follows: as the pressure increases from 0.5 MPa to 2.5 MPa, both micropore and mesopore specific surface areas show a downward trend, reaching the minimum at 2.5 MPa[32]. This is consistent with the influence trend of pressure on pyrolysis characteristics in thermogravimetric analysis. Under low pressure, gas adsorption occupies the active adsorption sites within micropores and mesopores, reducing the detectable specific surface area. Under high pressure, the gas adsorption-desorption process damages the coal structure, leading to a relative decrease in the number of micropores and mesopores, resulting in a further decrease in their specific surface areas. The macropore specific surface area does not change significantly with pressure, indicating that pressure has little effect on the macropore structure.

From the pore volume data under different adsorption temperatures and pressures in Figure 10, it can be seen that the pore volume distribution of the coal sample is similar to the specific surface area distribution. The mesopore volume accounts for more than 50% of the total pore volume. The influence of temperature on pore volume is as follows: as the temperature increases from 30 ℃ to 120 ℃, the micropore, mesopore, and macropore volumes of the coal sample exhibit distinct differential changes, a trend further modulated by the influence of adsorption pressure. Micropores show an overall fluctuating downward trend. The total decreases from 30 ℃ to 120 ℃ under 0.5MPa, 1.5MPa, and 2.5MPa are 19.4%, 20.9%, and 30.8% respectively. After reaching the minimum at 60 ℃ or 90 ℃, the volume slightly rebounds at 120 ℃. The attenuation is more severe under high pressure: micropores tend to be nearly occluded at 2.5MPa and 90 ℃, recording a minimal volume of only 0.009 cm³/g. Mesopore volume exhibit non-monotonic fluctuation characteristics. They undergoes an overall reduction of 15.6% and 16.5% respectively under low pressure (0.5MPa) and high pressure (2.5MPa) respectively, dropping to the lowest at 90 ℃ before rebounding at 120 ℃. Under medium pressure (1.5MPa), an anomalous increase observed at 90 ℃, reaching 9.091 cm³/g (167.7% higher than at 30 ℃), followed by a sharp drop to 3.002 cm³/g. Macropore volume is less susceptible to variations in adsorption pressure. They show a slow increasing trend with increasing temperature, with total increases of 5.2%, 10.5%, and 3.8% from 30 ℃ to 120 ℃ under 0.5MPa, 1.5MPa, and 2.5MPa respectively. The volume peaks at 90 ℃ or 120 ℃ with an extremely narrow variation range. The influence of pressure on pore volume is as follows: as the pressure increases from 0.5MPa to 2.5MPa, the total micropore volume shows a continuous downward trend. The total decreases from 0.5MPa to 2.5MPa at 30 ℃, 60 ℃, 90 ℃, and 120 ℃ are 80.6%, 81.2%, 97.1%, and 83.3% respectively. Micropores tend to be nearly fully occluded at 90 ℃ and 2.5MPa (only 0.009 cm³/g), and the shrinkage degree of micropores becomes increasingly pronounced with increasing pressure in all temperature groups. The change in mesopore volume shows temperature-dependent differences. It decreases continuously with increasing pressure at 30 ℃, 60 ℃, and 120 ℃, with decreases of 66.6%, 71.6%, and 68.8% from 0.5MPa to 2.5MPa respectively. At 90 ℃, it exhibits an anomalous "decrease-then-increase" trend: the mesopore volume increases to 9.091 cm³/g at 1.5MPa (1.77 times that recorded at 0.5MPa) and then declines sharply to 1.035 cm³/g at 2.5MPa (a decrease of 88.6% compared with 1.5MPa). Macropores are less affected by pressure. The variation range from 0.5MPa to 2.5MPa is less than 25% in all temperature groups. They show a slow downward trend at 30 ℃ and 60 ℃, and a slight fluctuating upward trend at 90 ℃ and 120 ℃, maintaining relative stability with a fluctuation range of 0.816~1.634 cm³/g.

3.5. Field Application

Based on the comprehensive analysis results of adsorption-desorption characteristics, thermogravimetric properties, and pore structure of coal samples collected from Xiaohuigou Coal Mine, integrated with the actual mining conditions of the 2201 mining face in the mine, the concept of "pressure-desorption capacity coordinated regulation" was applied to the optimization of gas extraction parameters. The 2201 mining face of Xiaohuigou Coal Mine is located in the eastern wing of the first mining area and is one of the key production faces of the mine. It adopts a U-type ventilation system and mainly mines the No. 2 coal seam. The coal seam is stable and minable throughout the region, with a thickness of 1.20-3.47 m (average 2.60 m) and a simple structure. The coal sample exhibits the proximate analysis characteristics of low moisture content, low ash content, low volatile matter content, and high fixed carbon content and the elemental composition characteristics of high carbon content, medium hydrogen content, and low nitrogen content, and possesses a high metamorphic grade, classifying it as a lean coal or meager coal. The mine faces problems such as high gas content, high gas pressure, unstable gas emission intensity, prominent gas over-limit at the upper corner, combustible and explosive coal dust[33]. Although it is classified as a non-spontaneously combustible coal seam, the risk of spontaneous combustion of residual coal in goaf still needs to be prevented and controlled.

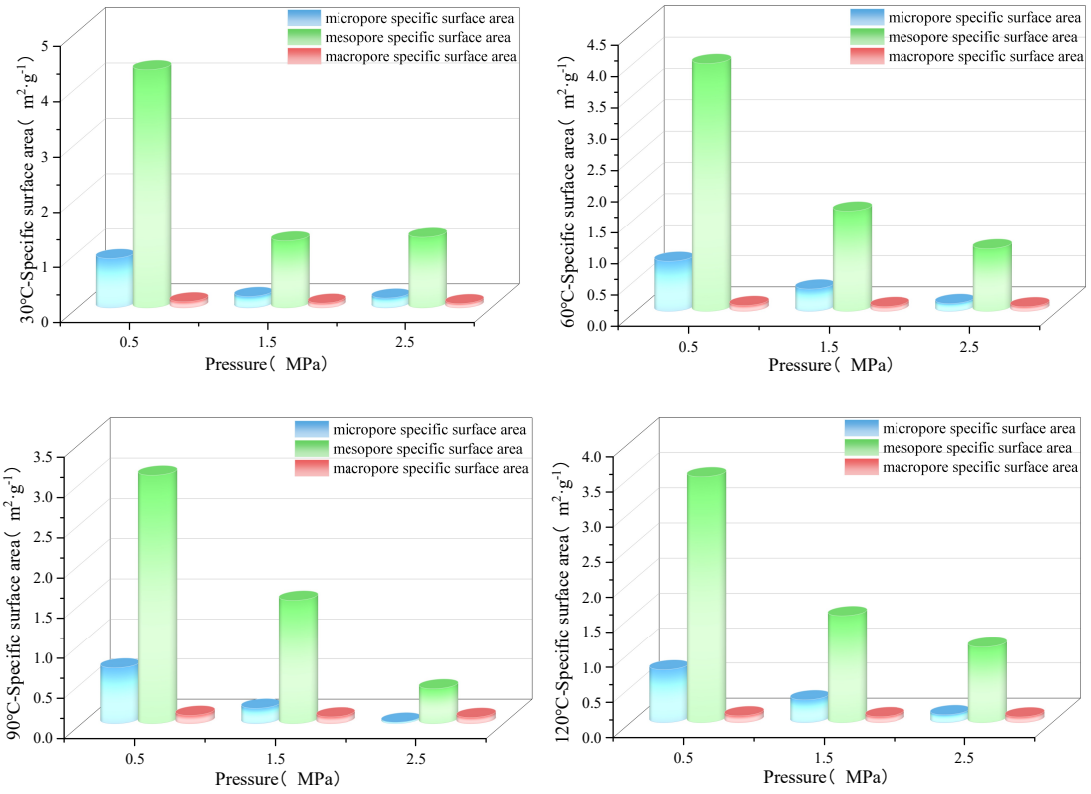

(a) Pore specific surface area at different adsorption temperatures

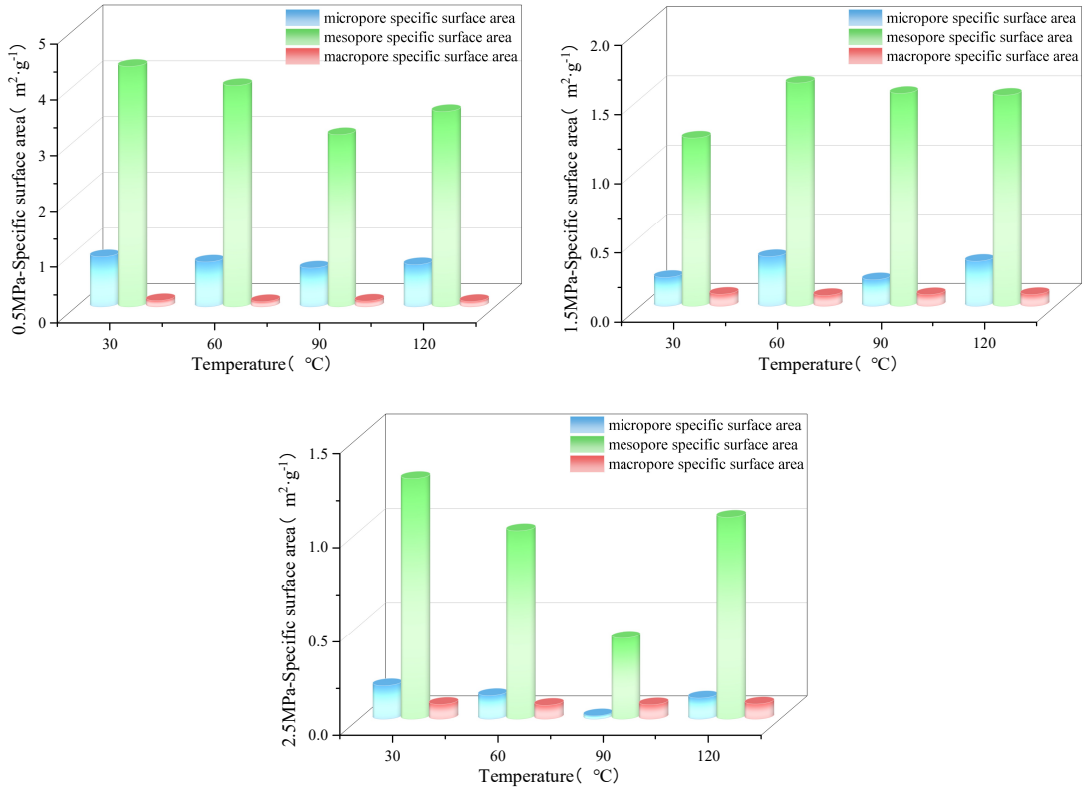

(b) Pore specific surface area at different adsorption pressures

Figure 9. Pore specific surface area

10.57647/ijeee.2025.1603.13

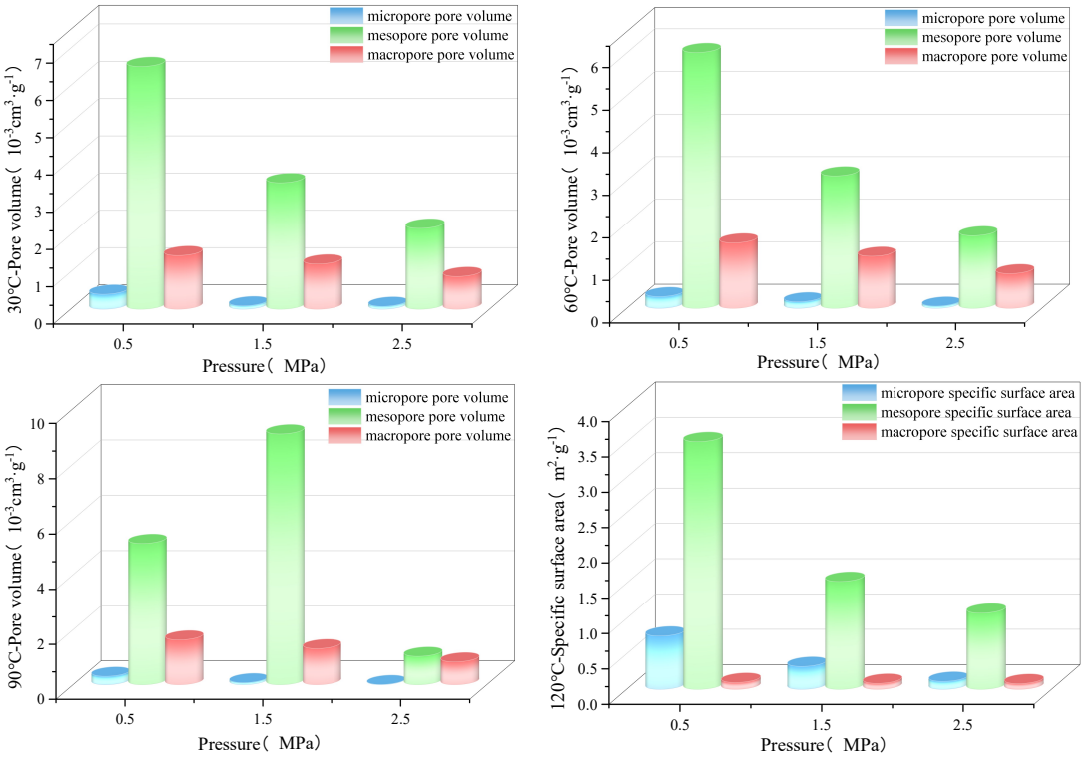

(a) Pore volume at different adsorption temperatures

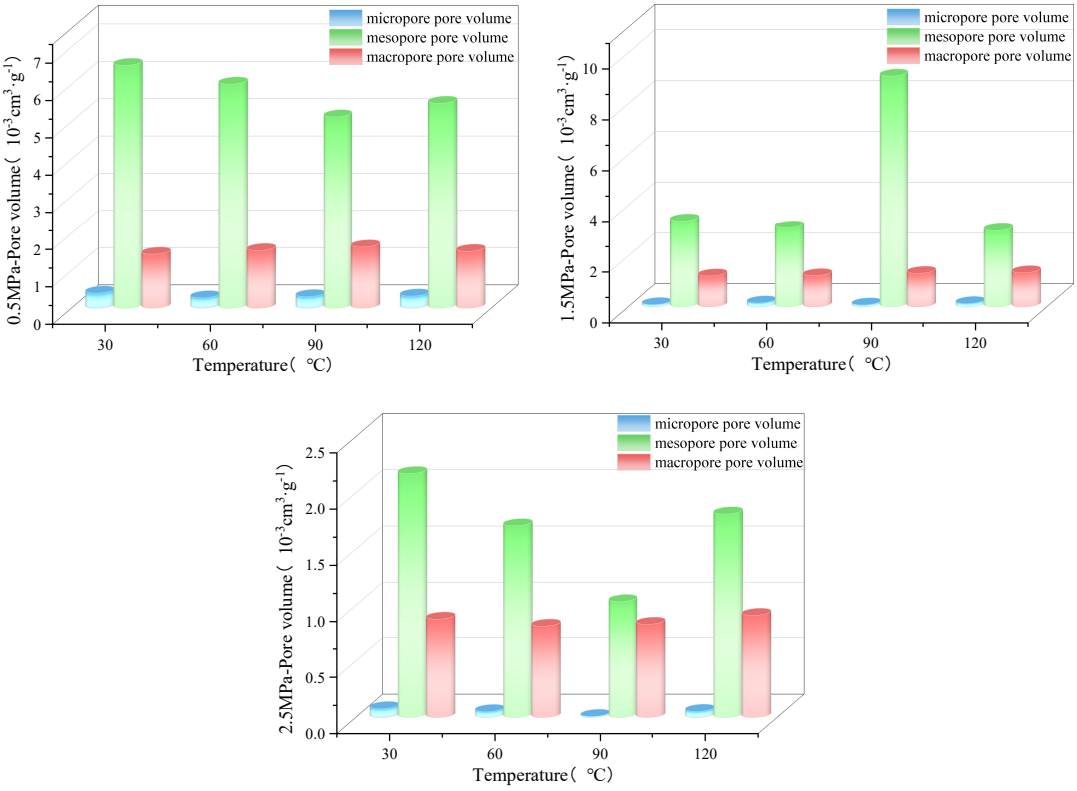

(b) Pore volume at different adsorption pressures

Figure 10. Pore volume

3.5.1. Setting and Implementation of Gas Extraction Parameters

The field-applied large-diameter borehole gas extraction technology was adopted, using a ZDJ10000L large-diameter drilling rig configured with Φ550 mm helical drill rods and Φ580 mm helical drill bits. Twelve large-diameter boreholes were constructed in the 2201 extraction roadway, with a borehole diameter of 580 mm, an borehole collar elevation of 1.2-1.8 m, an inclination angle of -1°~8°, and a length of 16 m, drilled perpendicular to the strike of the coal pillar with a spacing of 12-40 m. The total engineering volume is 180 m. The borehole construction followed the principle of "one borehole, one customized design; one borehole, one dedicated construction plan". Drilling parameters were optimized according to the differences in coal and rock properties: For coal boreholes: torque 6000-7000 N·m, rotational speed 40-55 r/min, feeding pressure 9-12 MPa, feeding force 140-160 kN; For rock boreholes: torque 7000-9000 N·m, rotational speed 30-40 r/min, feeding pressure 13-15 MPa, feeding force 170-180 kN. One-pass hole forming was achieved, and no construction anomalies such as borehole collapse or borehole abandonment were encountered during construction. The construction time of a single borehole was only 4 hours. Casing pipes with Φ426 mm diameter, 0.8 m length, and 3 mm wall thickness were used, jointed via internal socket connections and pushed into the borehole section by section through the drilling rig's thrust to accomplish borehole stabilization. The borehole sealing process adopted a combined technique of "cement mortar sealing at the borehole collar + pressure-injected polyurethane sealing in the inner section": the hole mouth was sealed with 0.5 m of cement mortar, and the inner section was sealed with 6 m of polyurethane (3 m at both ends) at a grouting pressure of 1.0MPa.

The polyurethane expansion ratio exceeds 50 times, which can rapidly secure the casing pipes and effectively seal gaps. For zones with complex geological structures, shotcreting was performed around the boreholes to prevent gas leakage. In terms of gas extraction pipeline connection, the pipeline diameter matching was optimized in a targeted manner. Φ450 mm connecting pipes were used to connect the Φ426 mm boreholes with the Φ630 mm main extraction pipelines, realizing a gradual diameter enlargement from boreholes to connecting pipes to the main pipeline. This avoids the "bottleneck" phenomenon and ensures stable extraction flow. Meanwhile, the gas extraction flow rate was controlled to not exceed 224 m³/min, and the negative pressure was maintained at 8 kPa, achieving low-negative-pressure, large-flow gas extraction mode to ensure extraction efficiency. The specific extraction design and on-site test results are presented in Figure 11.

3.5.2. *Investigation and Verification of Extraction Effect*

The influence range of large-diameter borehole extraction was investigated through group shutdown tests. The results show that within the advance distance range of 30-50 m from the working face, the gas extraction concentration and net flow show a continuous increasing trend; beyond 50 m, the growth trend gradually slows down, indicating that the effective influence range of large-diameter borehole gas extraction is 30-50 m. By comparing the extraction effects between large-diameter boreholes and Φ113 mm cross-boreholes: when the 5# large-diameter borehole is connected in parallel with 80 Φ113 mm cross-boreholes for extraction, the average gas extraction concentration of the Φ630 mm pipeline is 2.92%, the mixed flow rate is 143.21 m³/min, and the net gas flow rate is 4.29 m³/min. After independently shutting down the No. 5 large-diameter borehole, only 80 Φ113 mm cross-boreholes are used for extraction. The average extraction concentration drops to 1.43%, the mixed flow rate is 34.88 m³/min, and the net flow rate is 0.52 m³/min. Calculations show that the net gas flow rate of a single large-diameter borehole (3.77 m³/min) is equivalent to the extraction effect of 580 Φ113 mm cross-boreholes, significantly improving extraction efficiency. As the number of combined large-diameter boreholes increases, the working face production output and gas control effect are synergistically optimized: When 1 borehole is used for extraction, the maximum gas concentration at the upper corner is 0.28%, and the maximum daily output is 3468 t; When 4 boreholes are used for combined extraction, the maximum gas concentration at the upper corner is 0.56%, and the maximum daily output reaches 9370 t.

High-intensity mining of the working face is realized on the premise that the maintaining gas concentrations below the regulatory limit. During the gas extraction performance evaluation period, the cumulative net gas extraction volume via large-diameter boreholes reached 7.01×10^5 m³, with an average gas extraction concentration of 2.24% and an average mixed gas flow rate of the extraction system 166.3 m³/min. The average gas concentration in the 2201 mining face was 0.32%, while that at the upper corner of the working face averaged 0.40% (maximum: 0.67%), all of which were strictly maintained within the limits specified in the Coal Mine Safety Regulations.

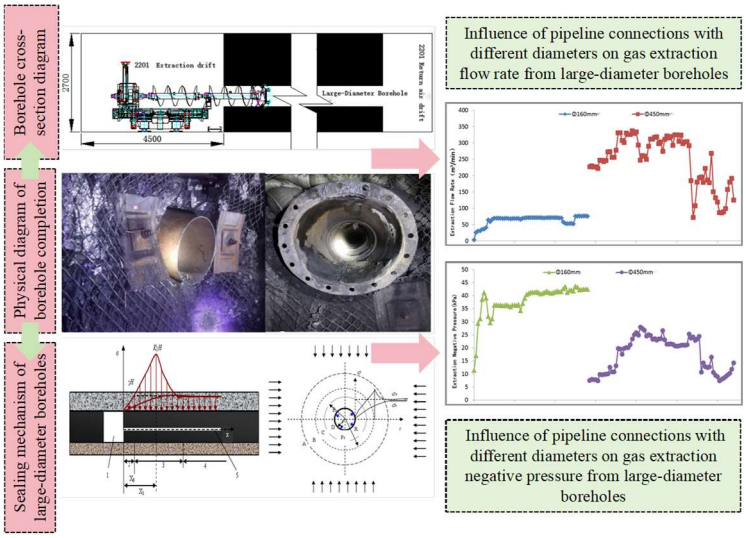

Figure 11. Extraction design and on-site test results

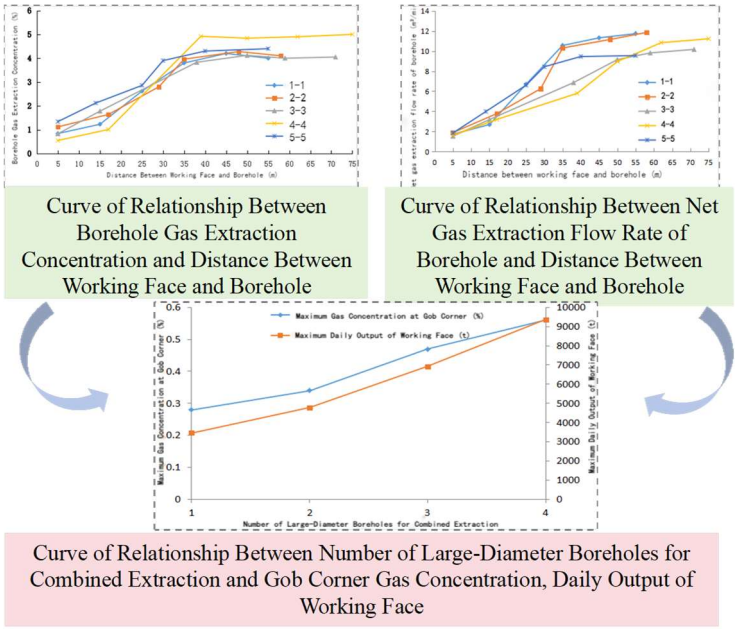

Figure 12. Verification results of gas extraction effect

Notably, during the initial weighting stage of the working face—when the roof remained intact and no fracture network had yet been formed—the gas extraction concentration of large-diameter boreholes was stably maintained within the range of 1.95%–12.40%. This effectively addressed the long-standing challenge of gas overrun at the upper corner during this critical stage.

4. Conclusions

(1) The coal samples from No.2 coal seam of Xiaohuigou Coal Mine exhibit the proximate analysis characteristics of “low moisture content, low ash content, low volatile matter content, and high fixed carbon content” and the elemental composition characteristics of "high carbon, medium hydrogen, and low nitrogen", classifying it as lean coal with a high metamorphic grade. Adsorption-desorption experiments indicate that temperature and pressure have a significant coupling effect on gas desorption capacity. Under the same initial pressure, an increase in temperature inhibit gas desorption—the maximum desorption capacity a 120 ℃ decreases by 20.35% compared with that at 30 ℃. Under the same temperature, the higher the initial pressure, the larger the desorption capacity—the maximum desorption capacity at 2.5MPa increases by 50.44% compared with that at 0.5MPa. Additionally, the adsorption equilibrium time is prolonged with increasing initial pressure and shortens with increasing temperature.

(2) Thermogravimetric and pore structure analyzes reveal that the coal pyrolysis process is divided into three stages: drying and dehydration stage (room temperature-200 ℃), pyrolysis and devolatilization weight loss stage

(200-600 ℃), and char combustion stage (600-800 ℃), with the concentrated volatile matter release temperature around 465 ℃. An increase in the adsorption temperature promotes the pyrolysis weight loss process, with the total weight loss rate reaching 31.13% at the adsorption temperature of 120 ℃. The influence of adsorption pressure on coal pyrolysis follows the trend that adsorption pressure inhibits pyrolysis at the low-pressure stage and promotes it at the high-pressure stage—this pattern avoids the misinterpretation that "higher pressure always enhances promotion". The pore structure is dominated by mesopores and macropores—high temperature causes micropore shrinkage, while high pressure leads to pore compression. The gas adsorption capacity and specific surface area of coal samples under low pressure (0.5 MPa) are significantly higher than those under high pressure conditions (1.5 MPa, 2.5 MPa).

(3) The optimized large-diameter borehole gas extraction technology (borehole diameter: 580 mm; grouting pressure: 1.5-2.0 MPa; negative pressure: 8 kPa) based on experimental results has achieved remarkable on-site application effects. It not only effectively controls the gas concentration at the upper corner of the working face but also achieves a gas extraction efficiency by 580 times compared with traditional cross-boreholes, with a cumulative net gas extraction volume exceeding 700,000 m³ during the performance evaluation period. Meanwhile, the risk of spontaneous combustion of residual coal in goafs is effectively prevented and controlled by means of "arranging boreholes in the heat dissipation zone of goafs+ controlling the advancing speed".

Funding

This study was funded by the National Natural Science Foundation of China [Grant Nos. 52574306, U25A20274, 52174230, U23B2094]. The authors extend their gratitude to Mr. Gao Jilong (from Scientific Compass www.shiyanjia.com) for providing invaluable assistance with the TG analysis.

Authors Contribution

All authors contributed to the study conception and design. Material preparation, data collection, and analysis were performed by Yongming Zou, Yaolin Cao, Jie Kang, Yuntao Liang, Congna Hao, Linlin Ding and Fuchao Tian .

The first draft of the manuscript was written by Yongming Zou, and all the authors commented on previous versions of the manuscript. All the authors read and approved the final manuscript.

Availability of data and materials

Data will be made available on request.

Conflict of interests

The authors have no relevant financial or conferential interests to disclose.

References

[1]. Wang S. M., Shen Y .J., Song S .J., et al. Changes in the Status of Coal Energy and Its Green and Low-Carbon Development Under the "Dual Carbon" Goals. Journal of China Coal Society, 2023, 48 (7): 2599-2612.
DOI: https://doi.org/10.13225/j.cnki.jccs.CN23.0260

[2]. Xuelong L, Shaojie C, Enyuan W, et al. Rockburst mechanism in coal rock with structural surface and the microseismic (MS) and electromagnetic radiation (EMR) response. Engineering Failure Analysis, 2021,124.
DOI: https://doi.org/10.1016/J.ENGFAILANAL.2021.105396

[3]. Tian F.C., Jia D.X., Chen M.Y., et al. Research Progress on the Characteristics of Spontaneous Combustion of Gas-Bearing Coal Under the Compound Disaster Environment of Goaf. Journal of China Coal Society, 2024, 49 (6): 2711-2727.
DOI: https://doi.org/10.13225/j.cnki.jccs.2023.0855

[4]. Chen L.Y., Li X.J., Shen Z.H., et al. Study on the Pore Structure and Fractal Characteristics of Outburst-Prone Coal in Northern Guizhou. China Safety Science Journal, 2020, 30 (2): 7.
DOI: https://doi.org/110.16265/j.cnki.issn1003-3033.2020.02.011

[5]. Wang L., Liu H.Q., Xie G.X., et al. Refined Characterization of Pore-Fracture Structure and Strength Deterioration Mechanism of Gas-Bearing Coal. Rock and Soil Mechanics, 2021, 42 (12): 3203-3216.
DOI: https://doi.org/10.16285/j.rsm.2021.1039

[6]. Shuang H. Q., Cui M. W., Li S. G., et al. Study on the In-situ Stress Distribution in Chenghe Mining Area and Its Influence on Gas Occurrence. Journal of Safety Science and Technology of China, 2025, 10 (21): 96-105.
DOI: https://doi.org/10.11731/j.issn.1673-193x.2025.10.012

[7]. Xu H.M.. Study on the Influence Laws of Temperature and Pressure on Gas Adsorption and Desorption of Coal Samples. Coal Mine Safety, 2014, 12 (33): 5-8.
DOI: https://doi.org/10.3969/i.issn.1005-2798.2024.12.002

[8]. Liu P., Chen W.P., Nie B.S., et al. Study on Pore Modification of Coal Mass by Broadband Ultrasonic Excitation and Its Regulation Mechanism on Gas Desorption Behavior. Journal of China Coal Society, 2025, 1 (1): 1-16.
DOI: https://doi.org/10.13225/j.cnki.jccs.CQ25.0931

[9]. Yan M., Long H., Bai Y., et al. Experimental Study on the Influence of Temperature Effect on the Adsorption and Desorption Characteristics of Coal Seam Gas. Mining Safety, 2019 , 3 (46): 6-10.

[10]. Li Z.R., Tian F.C., Wang G., et al. Microscopic Fractal Characteristics of Spontaneous Combustion of Gas-Bearing Coal Under Different Temperatures and Adsorption Pressures. Journal of Coal Science and Technology,2025,53(5):213-232.
DOI: https://doi.org/10.12438/cst.2024-0354

[11]. Niroj Kumar Mohalik S M S K. TGA/DSC study to characterise and classify coal seams conforming to susceptibility towards spontaneous combustion. International Journal of Mining Science and Technology, 2022, 1 (32): 75-88.
DOI: https://doi.org/10.1016/j.ijmst.2021.12.002

[12]. Nevin Selcuk N S Y. Combustion behaviour of Turkish lignite in O_2/N_2 and O_2/CO_2 mixtures by using TGA-FTIR. Journal of Analytical and Applied Pyrolysis, 2011, 2 (90): 133-139.
DOI: https://doi.org/10.1016/j.jaap.2010.11.003

[13]. Li S, Tian F, Jiang W, et al. Experimental investigation on coal desorption characteristics and spontaneous combustion properties evolution under the coupled effect of temperature and pressure[J]. Fuel, 2023, 351 (000): 11.
DOI: https://doi.org/10.1016/j.fuel.2023.128829

[14]. Zhou X.Q.. Effects of Degassing Temperature and Particle Size on Pore Structure and Adsorption Properties of Coals with Different Metamorphic Degrees. Jiaozuo: Henan Polytechnic University, 2023.
DOI: https://doi.org/10.27116/d.cnki.gjzgc.2023.001030

[15]. Zhou Y.. Study on the Main Controlling Factors of Coal Reservoir Pores and the Relationship with Gas-Bearing Property in Typical Mining Areas of Medium-Rank Coal in Liupanshui and High-Rank Coal in Bijie. Guiyang: Guizhou University, 2024.
DOI: https://doi.org/10.27047/d.cnki.ggudu.2024.001532

[16]. Li X.J., Shen Z.H., Li W.W., et al. Exploration and Development Potential of Shale Gas in the Niutitang Formation, Fenggang Area, Northern Guizhou. Natural Gas Industry, 2016, 36 (12): 72-79.
DOI: https://doi.org/10.3787/j.issn.1000-0976.2016.12.010

[17]. Tian F.C., Li Z.R., Li S.K., et al. Study on the Evolutionary Characteristics of Desorption and Spontaneous Combustion of Gas-Bearing Coal Under High Temperature and High Pressure Conditions. Coal Science & Technology (0253-2336), 2024, 52 (7): 101-113.
DOI: https://doi.org/10.12438/cst.2023-1046

[18]. Li F, Jiang B, Cheng G, et al. Methane Adsorption Behavior and Energy Variations of Brittle Tectonically Deformed Coal under High Temperature and High Pressure. ACS omega, 2022, 7 (3): 2737-2751.
DOI: https://doi.org/10.1021/acsomega.1c05383

[19]. Yang Y, Yu K, Ju Y, et al. Investigation on the Structure and Fractal Characteristics of Nanopores in High-Rank Coal: Implications for the Methane Adsorption Capacity. Journal of nanoscience and nanotechnology, 2021, 21 (1): 392-404.
DOI: https://doi.org/10.1166/jnn.2021.18513

[20]. Ma S, Wang Z, Wang L, et al. Inhibition mechanism and diffusion model of gas desorption in cylindrical coal core during frozen coring: Experimental simulation and validation[J]. Fuel, 2025,400:135779.
DOI: https://doi.org/10.1016/J.FUEL.2025.135779

[21]. Fu X, Liu X, Wu Q, et al. Characterization of Coal Particle Methane Desorption and Optimization of Desorption Model Based on Desorption Damage. ACS omega, 2024, 9 (8): 9170-9184.
DOI: https://doi.org/10.1166/jnn.2021.18513

[22]. Jia T, Liu C, Wei G, et al. Micro-Nanostructure of Coal and Adsorption-Diffusion Characteristics of Methane. Journal of nanoscience and nanotechnology, 2021, 21 (1): 422-430.
DOI: https://doi.org/10.1166/jnn.2021.18733

[23]. Ma S J, Wang Z F, Ren H Y, et al. Study on gas adsorption process of coal at low and variable temperature. China Safety Science Journal, 2019,29(10):124-129.
DOI: https://doi.org/10.16265/j.cnki.issn1003-3033.2019.10.019

[24]. Lei Shi Q L X G. Pyrolysis behavior and bonding information of coal — A TGA stud. Fuel Processing Technology, 2013, 1 (108): 125-132.
DOI: https://doi.org/10.1016/j.fuproc.2012.06.023

[25]. Li X, Zhao D, Li X, et al. Heat-dependent properties of methane diffusion in coal: an experimental study and mechanistic analysis. Environmental science and pollution research international, 2024, 31 (44): 56153-56173.
DOI: https://doi.org/10.1016/j.fuproc.2012.06.023

[26]. Krishna Kant Dwivedi E P S M K. A comparative study on pyrolysis characteristics of bituminous coal and low-rank coal using thermogravimetric analysis (TGA). International Journal of Coal Preparation and Utilization, 2019, 1 (42): 1-11.
DOI: https://doi.org/10.1080/19392699.2019.1566130

[27]. Wu Y.L., Ma J.W., Zhang W.L., et al. Study on the Characterization of Pore Structure of Tectonically Deformed Coal with Different Damage Types and Its Influence on Gas Desorption and Diffusion. Coal Science and Technology, 2025, 5 (46): 46-52.
DOI: https://doi.org/10.19896/j.cnki.mtki.2025.05.009

[28]. P S, A L, M L, et al. Mineralogical influence of mining intrusions in CFB combustion of Indian lignite. International Journal of Energy and Environmental Engineering, 2013, 4 (34): 1-11.
DOI: https://doi.org/10.1007/s40095-019-00331-2

[29]. Jin Y., Li D., Liu Y., et al. Study on Pyrolysis and Oxidation Characteristics of Coal Gangue Based on TGA-DSC. ACS omega, 2024, 9 (12): 14174-14186.
DOI: https://doi.org/10.1021/acsomega.3c09743

[30]. Cheng Y.P., Jiang J.Y.. Study on the Influence of Magmatic Rock Intrusion on the Micropore Characteristics of Coal Reservoirs in Huaibei Mining Area. Journal of China Coal Society, 2012, 4 (37): 634-640.
DOI: https://doi.org/10.13225/j.cnki.jccs.2012.04.027

[31]. Yuan A., Wang R., Yang X., et al. Integrated pore structure analysis and methane adsorption and desorption investigation in deep multi seam coal systems. Scientific reports, 2025, 15 (1): 34102.
DOI: https://doi.org/10.1038/s41598-025-19347-2

[32]. Shumin L, Haitao S, Dongming Z, et al. Experimental study of effect of liquid nitrogen cold soaking on coal pore structure and fractal characteristics[J]. Energy, 2023,275.
DOI: https://doi.org/10.1016/J.ENERGY.2023.127470

[33]. Gao M.. Gas Disaster Control and Ventilation System Design in Coal Mines. Energy and Energy Conservation, 2025, 1 (5): 75-78.
DOI: https://doi.org/10.16643/j.cnki.14-1360/td.2025.05.067